

Unusual Protonation-Induced Continuous Tunability of Optical Properties and Electroluminescence of a π -Conjugated Heterocyclic Oligomer

Jessica M. Hancock and Samson A. Jenekhe*

Department of Chemical Engineering and Department of Chemistry, University of Washington, Seattle, Washington 98195-1750

Received July 16, 2008

Revised Manuscript Received August 21, 2008

π -Conjugated organic and polymer semiconductors remain of great interest for use as light emitters and charge transporters in organic light-emitting diodes (OLEDs) for display and lighting applications.^{1,2} Additionally, they are of growing interest for use in developing chemical sensors since they can undergo analyte-induced shifts in their absorption and emission bands and/or significant variation in their fluorescence efficiency.^{3–10} One of the key advantages of organic and polymer semiconductors is the wide range of tunability of their optical, charge transport, and optoelectronic properties, usually by chemical synthesis. Conjugated oligomers and polymers containing basic nitrogen atoms also offer the possibility of facile modification of their optical and optoelectronic properties by protonation or metal ion complexation.^{4–10} However, the use of protonation as a means to tune electroluminescence and solid-state optoelectronic properties is yet to be fully exploited.⁵

In this Communication, we report observation of unusual protonation-induced continuous tunability in the optical and optoelectronic properties of a π -conjugated heterocyclic oligomer. We have found that progressive complexation of 6,6'-bis(2-(1-pyrenyl)-4-octylquinoline) (BPYQ, Figure 1a) by camphorsulfonic acid (CSA) generates a series of highly emissive materials (BPYQ:*n*CSA, where *n* > 0) with solid-state photoluminescence and electroluminescence spanning the visible region (477–612 nm). We demonstrate that efficient electroluminescence (845–1475 cd/m² and 0.43–1.44 cd/A) can be achieved at 477, 480, 540, 552, and 586–591 nm from the same π -conjugated oligomer in different protonated states.

CSA is a widely used complexing agent for the protonic acid doping of polyanilines, resulting in highly conducting polymers in which luminescence is completely quenched.¹¹ In general, similar small molecule and polymeric protonic acid doping of other heteroaromatic polymers has been used as a way of producing electrically conducting polymers that do not exhibit luminescent properties.^{11,12} There has only been one report of electroluminescence in a protonated organic semiconductor. Monkman et al. reported orange electroluminescence of a polypyridine protonated by CSA and observed low external quantum efficiency (0.02%) with no reported brightness.⁵

The synthesis, photophysics, and electroluminescence of oligoquinolines end-capped with various aromatic end groups have been previously reported by our group; however, the effects of protonation were not explored.¹³ The synthesis of BPYQ is shown in Scheme S1 of the Supporting Information, and the structure was confirmed by mass spectrometry, ¹H NMR spectra (Figure S1), and absorption/emission spectra.^{13a} A photograph of chloroform solutions of BPYQ with various amounts of

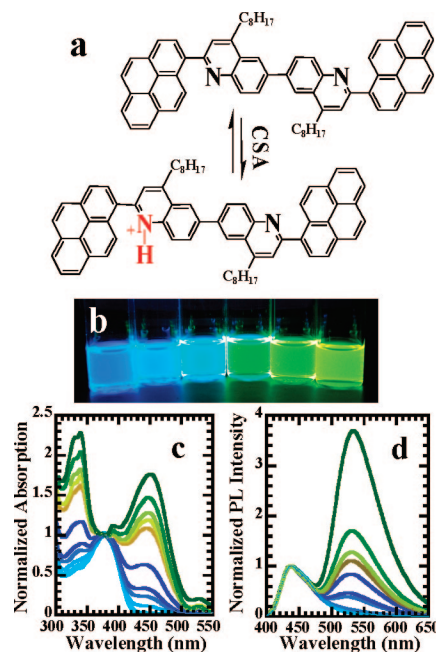


Figure 1. (a) Molecular structure of BPYQ and its singly protonated form. (b) Photograph of chloroform solutions of BPYQ containing various molar ratios of CSA (BPYQ:CSA = 1:0 to 1:27) under UV irradiation. Normalized optical absorption spectra (c) and PL emission spectra (d) of BPYQ:CSA in chloroform shown in (b).

CSA, corresponding to the solutions for absorption and photoluminescence spectra, under UV irradiation is shown in Figure 1b. Blue to green emission is seen in the solutions. Figure 1c shows the normalized optical absorption spectra of chloroform solutions of various molar compositions of BPYQ:*n*CSA, where *n* ranges from 0 to 27. In chloroform solution, BPYQ has a maximum absorption ($\lambda_{\text{max}}^{\text{abs}}$) at 378 nm. Upon the addition of CSA, the relative intensity of the BPYQ absorption band decreases, and two new absorption bands corresponding to protonated BPYQ emerge at 341 and 452 nm. The relative intensities of the new absorption bands increase with increasing amounts of CSA. The Benesi–Hildebrand plot of the normalized absorbance of BPYQ:*n*CSA vs $1/c_{\text{CSA}}$, where c_{CSA} is the concentration of CSA, gave an excellent linear fit (Figure S2), indicating that only one of the quinoline moieties is protonated.¹⁴

The photoluminescence (PL) emission spectrum of BPYQ in chloroform, shown in Figure 1d, has a maximum ($\lambda_{\text{max}}^{\text{PL}}$) centered at 434 nm. Upon the addition of CSA, a new lower energy PL emission band emerges at 523–530 nm. The position of this PL emission band represents a significantly larger red shift compared to diphenylquinoline (PQ), whose $\lambda_{\text{max}}^{\text{PL}}$ of 413 nm is red-shifted by only 20 nm due to protonation.^{7a} The dual PL emission spectra of BPYQ:*n*CSA (Figure 1d) reflects BPYQ equilibrium between protonated and unprotonated forms of BPYQ, with photophysical characteristics of both in solution. Increasing the amount of CSA results in an increase in the relative green emission band (530 nm) of the protonated BPYQ to blue emission band (434 nm) of the neutral BPYQ. The photophysical properties of BPYQ:*n*CSA, where *n* = 0–27, are collected in Table S1, and the corresponding non-normalized optical absorption and PL emission spectra are included in Figure S3.

BPYQ has a PL quantum yield of 87%. Upon the addition of small molar equivalents of CSA (*n* = 0.2–2) the quantum

* Corresponding author. E-mail: jenekhe@u.washington.edu.

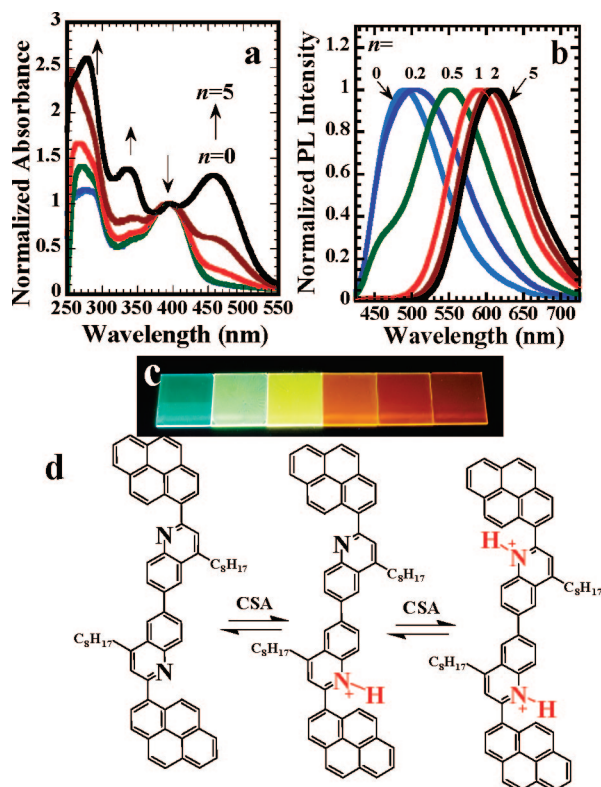


Figure 2. Normalized optical absorption spectra (a) and PL emission spectra (b) of BPYQO:*n*CSA thin films. (c) Photograph of thin films of BPYQO:*n*CSA under UV irradiation. (d) Molecular structure of BPYQO and its protonated forms.

yield is reduced to 77–85%, whereas the fluorescence is further quenched to 37–67% for $n = 5$ –27. It has been shown that the quinoline moiety maintains a high fluorescence quantum yield^{7c} and undergoes a moderate red shift in its optical absorption (16 nm) and PL emission (20–60 nm) following protonation.^{7a,c} The large protonation-induced red shift in the optical absorption (70 nm) and PL emission (92 nm) and the 57% decrease of the fluorescence quantum yield of BPYQO following complexation by CSA suggests that the optical response is not exclusive to the protonation of the oligoquinoline. Although excimer formation has been reported in protonated quinolines,^{7a,c} BPYQO:*n*CSA in dilute solution should preclude the close chromophore/chromophore interactions essential to excimer formation. Additionally, large red shifts in absorption (62 nm) and PL emission (77 nm) maxima have been observed in an alkoxy-substituted polypyridine due to protonation-mediated intramolecular hydrogen bonding (i.e., planarization).⁵ However, this is not what is observed in BPYQO:*n*CSA since there are no heteroatoms in the pyrene end groups that would facilitate hydrogen bonding with the protonated imine nitrogen on the quinolinium ion. We propose that intramolecular charge transfer between the quinolinium ion acceptor and the pyrenyl donor may explain the unique photophysical characteristics of BPYQO:*n*CSA.^{13c,e} Future work will include a detailed photophysical investigation of protonated species of oligoquinolines including the calculation of their electronic structures to fully understand the underlying phenomena.

Figure 2a shows the normalized optical absorption spectra of thin films of BPYQO:*n*CSA spin-coated from chloroform solutions where $n = 0, 0.2, 0.5, 1, 2$, and 5. The absorption of thin films of BPYQO has a $\lambda_{\text{max}}^{\text{abs}}$ at 394 nm. Upon the addition of CSA, two new bands emerge at 336 and 457 nm, and their relative intensities increase with increasing CSA content. The

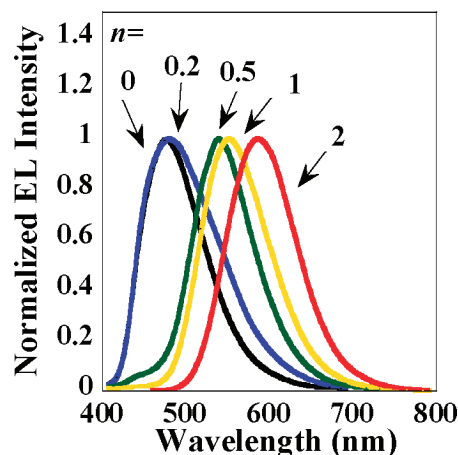


Figure 3. Electroluminescence emission spectra of BPYQO:*n*CSA-based OLEDs (ITO/PEDOT/PVK/BPYQO:*n*CSA/TPBI/LiF/Al) at 10 V for $n = 0, 0.2, 0.5, 1$ and 2.

normalized PL emission spectra of thin films of BPYQO:*n*CSA and a photograph of the films under UV irradiation are shown in parts b and c of Figure 2, respectively. These PL emission spectra clearly show that the degree of protonation and amount of CSA in BPYQO:*n*CSA is a means to tune the emission color from blue to green to yellow to red/orange (Figure 2b,c). PL emission maxima of 489, 505, 552, 590, 605, and 612 nm were achieved from thin films of BPYQO:*n*CSA; $n = 0, 0.2, 0.5, 1, 2$, and 5, respectively. Thus, for example, the PL emission of BPYQO:5CSA thin films is red-shifted by 123 nm compared to the pristine BPYQO. A remarkable feature of BPYQO:*n*CSA is the striking difference between the solution and thin film photoluminescence emission spectra. In solution, which is representative of the emission of BPYQO:*n*CSA with no intermolecular interactions, a dual blue (434 nm) and green (530 nm) emission is observed (Figure 1d). Changing the degree of protonation, i.e., increasing the amount of CSA, results in changes in the relative intensities of the dual peaks. However, in the solid state the PL emission of BPYQO:*n*CSA has only one band that can be tuned from blue to green to yellow to orange to red (Figure 2b), depending on the amount of CSA. We propose that in the solid state the dual PL emission bands seen in solution (434 and 530 nm) are largely fused into one relatively broad band at low CSA amounts ($n < 2$). In this case, the singly protonated BPYQO remains in equilibrium with the unprotonated oligomer. At sufficiently high concentrations of CSA in the solid state complex BPYQO:*n*CSA ($n \geq 2$), the PL emission is exclusively from the doubly protonated oligomer with emission peak in the 590–612 nm range. The molecular structures of the protonated forms of BPYQO in thin film are shown in Figure 2d.

The dramatic optical response observed in BPYQO:*n*CSA thin films suggested that protonation could be an effective method to tune electroluminescence of heterocyclic organic/polymer semiconductors over a wide range. We fabricated OLEDs based on BPYQO:*n*CSA with device architectures that included a hole transport layer, poly(*N*-vinylcarbazole) (PVK), and a hole blocking/electron transporting layer, 1,3,5-tris(*N*-phenylbenzimidazol-2-yl)benzene (TPBI), to improve charge injection and transport in the devices (ITO/PEDOT/PVK/BPYQO:*n*CSA/TPBI/LiF/Al). The electroluminescence (EL) spectra and the corresponding current density–voltage and luminance–voltage characteristics of the OLEDs are shown in Figures 3 and 4, respectively. Films of BPYQO:*n*CSA were spin-coated from their 0.5 wt % formic acid solutions because

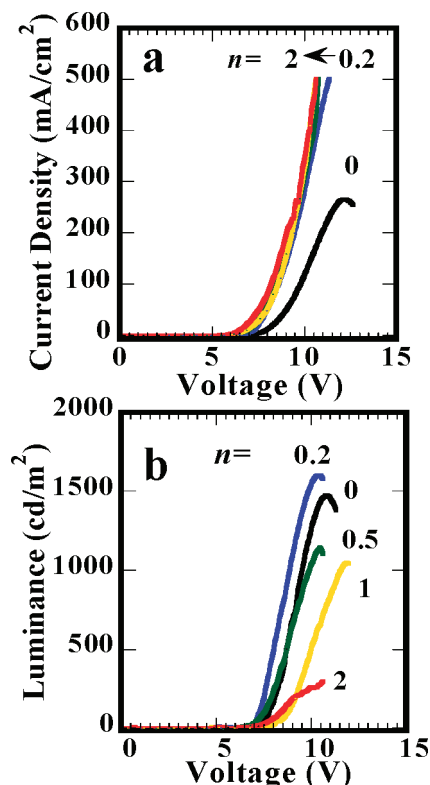


Figure 4. (a) Current density–voltage and (b) luminance–voltage characteristics of BPYQO:*n*CSA-based OLEDs (ITO/PEDOT/PVK/BPYQO:*n*CSA/TPBI/LiF/Al). The different curves are for *n* = 0, 0.2, 0.5, 1, and 2.

of the solubility of PVK in chloroform. The spin-coated thin films were dried overnight in a 60 °C vacuum oven to ensure complete evaporation of formic acid.

Blue electroluminescence was achieved from BPYQO, with an EL emission maxima ($\lambda_{\text{max}}^{\text{EL}}$) of 477 nm and CIE coordinates of (0.17, 0.27). This represents a 12 nm blue shift relative to the PL emission spectra of BPYQO thin films spin-coated from chloroform solution, confirming complete evaporation of formic acid during drying and that the EL emission originates from the pristine BPYQO. Small shifts in the EL emission spectra relative to PL emission spectra are commonly observed in OLEDs.¹³ The devices had a turn-on voltage (V_{on})¹⁵ of 5.1 V and a brightness of 1475 cd/m² with a luminous efficiency of 1.44 cd/A. Blue-green EL emission with a $\lambda_{\text{max}}^{\text{EL}}$ = 480 nm and CIE(0.20, 0.32) was observed from devices based on BPYQO:*n*CSA with a small amount of CSA, *n* = 0.2. The diodes had improved brightness (1600 cd/m²) and lower V_{on} (4.7 V) relative to diodes based on the pristine BPYQO, likely due to improved charge injection into the film; the luminous efficiency was still relatively high at 1.0 cd/A.

Devices based on BPYQO:*n*CSA, where *n* = 0.5 and 1, exhibited green-yellow ($\lambda_{\text{max}}^{\text{EL}}$ = 540 nm; CIE(0.34, 0.56)) and yellow ($\lambda_{\text{max}}^{\text{EL}}$ = 552 nm; CIE(0.41, 0.55)) EL emission, respectively. Brightnesses of 1045–1145 cd/m² were achieved, with efficiencies of 0.43–0.54 cd/A and V_{on} of 4.4 V. The EL emission was further red-shifted to 586 nm and CIE(0.52, 0.48) in OLEDs based on BPYQO:2CSA. This represents a 109 nm red shift relative to the EL emission spectrum of pristine BPYQO. These devices had brightnesses of 295 cd/m² with luminous efficiencies of 0.1 cd/A and a relatively lower V_{on} of 4.2 V. Interestingly, the turn-on voltage of the OLEDs decreased with increasing CSA content, suggesting that charge injection into the BPYQO:*n*CSA emission layer is improved with

increasing degree of protonation. This is evident when the current density–electric field characteristics of single-layer devices of the type ITO/PEDOT/BPYQO:*n*CSA/LiF/Al are compared (Figure S4, Supporting Information). The EL CIE coordinates of BPYQO:*n*CSA-based diodes are plotted in Figure S5.

Enhanced device performance was achieved in the orange/red-emitting devices by increasing the film thickness of the BPYQO:2CSA layer. These devices gave brightnesses as high as 845 cd/m² with luminous efficiencies of 0.6 cd/A and EL emission maxima at 591 nm (Figure S6). Additionally, the EL emission spectrum of BPYQO:2CSA was very stable; the emission spectra were identical over a wide range of applied voltages (Figure S6a). These results suggest that significantly improved device performance can be achieved from BPYQO:*n*CSA complexes upon further device optimization.

In conclusion, we have observed efficient photoluminescence and electroluminescence throughout the visible region by controlling the degree of protonation of a π -conjugated heterocyclic oligomer without synthetic modification. Electroluminescence from blue to yellow to red-orange color with stable emission spectra was realized with good device performance (845–1475 cd/m² and 0.43–1.44 cd/A) from the oligoquinoline/CSA complexes, BPYQO:*n*CSA. In solution, the observed dual blue (434 nm) and green (530 nm) emission comes from mixtures of the pristine and singly protonated species, respectively, whereas the doubly protonated species becomes the dominant orange/red emitter at sufficiently high amounts of CSA in the solid state. Among the significance of these results are (1) demonstration of protonation and acid complexation as a facile method to achieve efficient photoluminescence and electroluminescence spanning the visible region from an emissive heterocyclic oligomer semiconductor and (2) the observed large protonation-induced optical response demonstrates that fluorescent conjugated heterocyclic oligomers such as oligoquinolines are attractive candidates for use in stimuli-responsive light-emitting devices and chemical sensors. Future work will include investigation of other π -conjugated heterocyclic oligomers and polymers with the aim to fully understand the underlying phenomena while exploring applications in optoelectronics and sensors.

Acknowledgment. This research was supported by the NSF (DMR-0805259) and a UIF Nanotechnology Fellowship Award to J.M.H. from the Center of Nanotechnology. We thank Pei-Tzu Wu, Angela Gifford, and Christopher Tonzola for the synthesis of BPYQO.

Supporting Information Available: Synthesis and characterization of BPYQO; preparation of BPYQO:*n*CSA thin films and OLED device fabrication and testing; optical absorption and PL emission spectra and table of photophysical properties of BPYQO:*n*CSA; Benesi–Hildebrand plot for complexation of BPYQO with CSA; EL spectra and current density–luminance–voltage characteristics of BPYQO:2CSA OLEDs; current density–electric field plots and CIE coordinates of BPYQO:*n*CSA OLEDs. This material is available free of charge via the Internet at <http://pubs.acs.org>.

References and Notes

- (1) (a) See the special issue on Organic Electronics: *Chem. Mater.* **2004**, *16*, 4381–4846. (b) See the special issue on Organic Electronics and Optoelectronics: *Chem. Rev.* **2007**, *107*, 923–1386. (c) Kulkarni, A. P.; Tonzola, C. J.; Babel, A.; Jenekhe, S. A. *Chem. Mater.* **2004**, *16*, 4556. (d) Tang, C. W.; VanSlyke, S. A. *Appl. Phys. Lett.* **1987**, *51*, 913. (e) Friend, R. H.; Gymer, R. W.; Holmes, A. B.; Burroughs, J. H.; Marks, R. N.; Taliani, C.; Bradley, D. D. C.; Dos Santos, D. A.; Brédas, J. L.;

- Lögdlund, M.; Salaneck, W. R. *Nature (London)* **1999**, 397, 121. (f) Kraft, A.; Grimsdale, A. C.; Holmes, A. B. *Angew. Chem., Int. Ed.* **1998**, 37, 402. (g) Heeger, A. J. *Solid State Commun.* **1998**, 107, 673. (h) Hughes, G.; Bryce, M. R. *J. Mater. Chem.* **2005**, 15, 94.
- (2) (a) Hsieh, B. Y.; Chen, Y. *Macromolecules* **2007**, 40, 8913. (b) Niu, Q.; Zhou, Y.; Wang, L.; Peng, J.; Wang, J.; Pei, J.; Cao, Y. *Adv. Mater.* **2008**, 20, 964. (c) Cho, N. S.; Hwang, D.-H.; Jung, B.-J.; Lim, E.; Lee, J.; Shim, H.-K. *Macromolecules* **2004**, 37, 5265. (d) Ding, L.; Lu, Z.; Egbe, D. A. M.; Karasz, F. E. *Macromolecules* **2004**, 37, 1037. (e) Ananthakrishnan, N.; Padmanaban, G.; Ramakrishnan, S.; Reynolds, J. R. *Macromolecules* **2005**, 38, 7660.
- (3) (a) McQuade, D. T.; Pullen, A. E.; Swager, T. M. *Chem. Rev.* **2000**, 100, 2537. (b) Basabe-Desmonts, L.; Reinhoudt, D. N.; Crego-Calama, M. *Chem. Soc. Rev.* **2007**, 36, 993. (c) Thomas, S. W.; Joly, G. D.; Swager, T. M. *Chem. Rev.* **2007**, 107, 1339. (d) Ho, H.-A.; Boissinot, M.; Bergeron, M. G.; Corbeil, G.; Doré, K.; Boudreau, D.; Leclerc, M. *Angew. Chem., Int. Ed.* **2002**, 41, 1548. (e) Chen, L.; McBranch, D. W.; Wang, H.-L.; Helgeson, R.; Wudl, F.; Whitten, D. G. *Proc. Natl. Acad. Sci. U.S.A.* **1999**, 96, 12287. (f) Kumaraswamy, S.; Bergstedt, T.; Shi, X.; Rininsland, F.; Kushon, S.; Xia, W.; Ley, K.; Achyuthan, K.; McBranch, D.; Whitten, D.; Meyer, T. J. *Proc. Natl. Acad. Sci. U.S.A.* **2004**, 101, 7511. (g) Gaylord, B. S.; Heeger, A. J.; Bazan, G. C. *Proc. Natl. Acad. Sci. U.S.A.* **2002**, 99, 10954.
- (4) (a) Wang, C.; Kilitziraki, M.; MacBride, J. A. H.; Bryce, M. R.; Horsburgh, L. E.; Sheridan, A. K.; Monkman, A. P.; Samuel, I. D. W. *Adv. Mater.* **2000**, 12, 217. (b) Monkman, A. P.; Halim, M.; Samuel, I. D. W.; Horsburgh, L. E. *J. Chem. Phys.* **1998**, 109, 10372. (c) Liaw, D.-J.; Wang, K.-L.; Chang, F.-C. *Macromolecules* **2007**, 40, 3568. (d) Sun, M. *J. Chem. Phys.* **2006**, 124, 054903. (e) Kwon, T. W.; Alam, M. M.; Jenekhe, S. A. *Chem. Mater.* **2004**, 16, 4647.
- (5) Monkman, A. P.; Palsson, L.-O.; Higgins, R. W. T.; Wang, C.; Bryce, M. R.; Batsanov, A. S.; Howard, J. A. K. *J. Am. Chem. Soc.* **2002**, 124, 6049.
- (6) (a) Agrawal, A. K.; Jenekhe, S. A. *Chem. Mater.* **1993**, 5, 633. (b) Agrawal, A. K.; Jenekhe, S. A. *Macromolecules* **1993**, 26, 895. (c) Agrawal, A. K.; Jenekhe, S. A. *Chem. Mater.* **1992**, 4, 95. (d) Alam, M. M.; Zhu, Y.; Jenekhe, S. A. *Langmuir* **2003**, 19, 8625.
- (7) (a) Lu, L.; Jenekhe, S. A. *Macromolecules* **2001**, 34, 6249. (b) Economopoulos, S. P.; Andreopoulou, A. K.; Gregoriou, V. G.; Kallitsis, J. K. *Chem. Mater.* **2005**, 17, 1063. (c) Chochos, C. L.; Stefopoulos, A. A.; Campidelli, S.; Prato, M.; Gregoriou, V. G.; Kallitsis, J. K. *Macromolecules* **2008**, 41, 1825.
- (8) Bangcuyo, C. G.; Rampey-Vaughn, M. E.; Quan, L. T.; Angel, S. M.; Smith, M. D.; Bunz, U. H. F. *Macromolecules* **2002**, 35, 1563.
- (9) (a) Tong, H.; Wang, L.; Jing, X.; Wang, F. *Macromolecules* **2003**, 36, 2584. (b) Jenekhe, S. A.; Lu, L. D.; Alam, M. M. *Macromolecules* **2001**, 34, 7315.
- (10) (a) Wilson, J. N.; Bunz, U. H. F. *J. Am. Chem. Soc.* **2005**, 127, 4124. (b) Zuccherro, A. J.; Wilson, J. N.; Bunz, U. H. F. *J. Am. Chem. Soc.* **2006**, 128, 11872. (c) Spitler, E. L.; Shirtcliff, L. D.; Haley, M. M. *J. Org. Chem.* **2007**, 72, 86.
- (11) (a) Yoon, C.; Reghu, M.; Moses, D.; Heeger, A. J.; Cao, Y. *Synth. Met.* **1994**, 63, 47. (b) Yang, C. Y.; Cao, Y.; Smith, P.; Heeger, A. J. *Synth. Met.* **1993**, 53, 293.
- (12) (a) Groenendaal, L.; Jonas, F.; Freitag, D.; Pielartzik, H.; Reynolds, J. R. *Adv. Mater.* **2000**, 12, 481. (b) Alam, M. M.; Jenekhe, S. A. *J. Phys. Chem. B* **2002**, 106, 11172.
- (13) (a) Hancock, J. M.; Gifford, A. P.; Tonzola, C. J.; Jenekhe, S. A. *J. Phys. Chem. C* **2007**, 111, 6875. (b) Tonzola, C. J.; Kulkarni, A. P.; Gifford, A. P.; Kaminsky, W.; Jenekhe, S. A. *Adv. Funct. Mater.* **2007**, 17, 863. (c) Hancock, J. M.; Gifford, A. P.; Zhu, Y.; Lou, Y.; Jenekhe, S. A. *Chem. Mater.* **2006**, 18, 4924. (d) Tonzola, C. J.; Alam, M. M.; Jenekhe, S. A. *Macromolecules* **2005**, 38, 9539. (e) Hancock, J. M.; Gifford, A. P.; Champion, R. D.; Jenekhe, S. A. *Macromolecules* **2008**, 41, 3588.
- (14) Chu, Q.; Medvetz, A.; Pang, Y. *Chem. Mater.* **2007**, 19, 6421.
- (15) V_{on} is defined as the voltage at which EL emission is observed to the eye.

MA8016037